Pergamon

Int. J. Solids Structures Vol. 35, Nos 9–10, pp. 941–960, 1998

0020–7683/98 $19.00 + .00

PII: S0020–7683(97)–00090–S

MICROMECHANICS AND EFFECTIVE TRANSVERSE ELASTIC MODULI OF COMPOSITES WITH RANDOMLY LOCATED ALIGNED CIRCULAR FIBERS

J. W. JU† and X. D. ZHANG‡
Department of Civil and Environmental Engineering, University of California, Los Angeles, CA 90095, U.S.A.

(*Received* 8 *November* 1996; *in revised form* 19 *March* 1997)

Abstract—Based on the two-dimensional (plane-strain) micromechanical fiber interaction framework, effective transverse elastic moduli of two-phase brittle matrix composites containing many randomly located yet unidirectionally aligned circular fibers are investigated in this paper. The fibers are characterized as infinitely long and equal-sized inclusions. By employing the local pairwise fiber interaction formulation coupled with the ensemble-area averaged field equations, the proposed approximate analysis leads to a novel, higher-order (in fiber volume fraction), and accurate method for the prediction of effective transverse elastic moduli of two-phase fiber reinforced composites. In addition, the proposed micromechanical approach is extended to predict the effective transverse shear velocities of fiber suspensions with randomly located aligned rigid fibers. Comparisons with experimental data, Hashin's variational bounds, and improved three-point bounds are also presented to illustrate the predictive capability of the proposed method for fiber-reinforced composites. © 1997 Elsevier Science Ltd.

1. INTRODUCTION

Fiber reinforced composites (FRC) have been of interest to researchers and engineers for several decades owing to their superior mechanical performance over traditional materials. They provide many advantages such as weight savings, high stiffness/weight and strength/weight ratios, better environmental durability and resistance against corrosion and humidity, and so on. Applications of fiber reinforced composites have been made to aircraft, space shuttles, automobiles, sporting goods, and civil engineering structures (Mallick, 1993). Fiber reinforced composites can be described as a matrix reinforced by fibers of another material. The fibers could be short or long, aligned or randomly oriented, and periodically or randomly dispersed. Therefore, the prediction and estimation of effective properties of fiber reinforced composites are of great importance to engineers and researchers.

In this paper, we consider a linearly elastic isotropic matrix reinforced by linearly elastic, unidirectionally aligned, randomly located, impenetrable, and infinitely long *circular* fibers. The fibers could be isotropic or transversely isotropic. Furthermore, we assume that the composite specimen is: (a) statistically homogeneous and statistically transversely isotropic (Hashin, 1965; Ju and Chen, 1994a, 1994b); and (b) with perfect interfacial bonding between the matrix and fibers. The overall composite is therefore *transversely isotropic*. As shown in Fig. 1, the Cartesian coordinate system can be set up with axis 3 parallel to the fiber direction. The overall transverse isotropy can be characterized by five *effective* elastic moduli; namely, the plane-strain bulk modulus κ^*, the transverse shear modulus μ_T^*, the axial Young's modulus E_A^*, the axial Poisson's ratio ν_A^* and the axial shear modulus μ_A^*. Hill (1964) showed that there were only three independent effective elastic constants for such fibrous composites and the other two constants could be easily determined.

† Associate Professor and author to whom all correspondence should be addressed.
‡ Graduate Research Assistant.

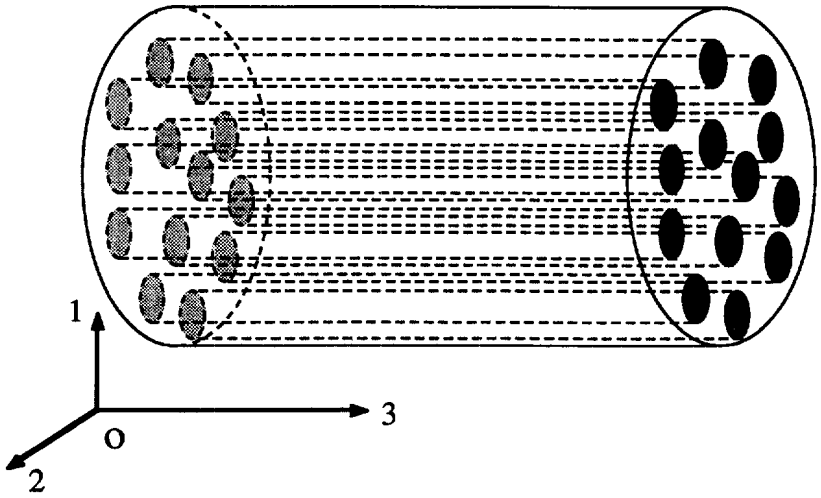

Fig. 1. Schematic plot of a composite reinforced by unidirectionally aligned yet randomly located long circular fibers.

Many theoretical methods have been developed in the literature to predict effective elastic moduli of fiber reinforced composites; see Hashin (1983), Mura (1987), Zhao and Weng (1990), and Nemat-Nasser and Mori (1993) for some literature reviews. The first school, stemming from the pioneering work of Hashin and Rosen (1964) and Hill (1964), employed variational principles or linear comparison composites to obtain mathematical lower and upper bounds for effective elastic, transversely isotropic moduli of fiber reinforced composites. Subsequently, Hashin (1965) derived the variational upper and lower bounds for the plane strain bulk modulus κ^*, and the transverse and axial shear moduli μ_T^* and μ_A^* of fiber reinforced composites with arbitrary transverse phase geometry in terms of constituent phase elastic moduli and phase volume fractions. Upper and lower bounds on effective axial Young's modulus E_A^* and axial Poisson's ratio ν_A^* were later derived by Hashin (1972). "Improved" third-order mathematical bounds, which depend on statistical microstructural information of random fiber composites, were derived by Silnutzer (1972) for μ_A^*, κ^* and μ_T^*. Moreover, Milton (1982) proposed the fourth-order bounds for the effective axial shear modulus μ_A^*; see also Torquato and Lado (1992) for detailed calculations on the third-order and fourth-order bounds. Nomura and Chou (1984) also proposed the third-order bounds based on variational principles and the three-point correlation functions. It is noted that the third-order bounds are narrower than the two-point bounds of Hashin's type.

The second school is known as the "effective medium approach" for micromechanical estimation of effective moduli of FRC. This category includes the self-consistent method (Kröner, 1958; Budiansky, 1965; Hill, 1965), the differential scheme (McLaughlin, 1977; Hashin, 1988), the generalized self-consistent method (Christensen and Lo, 1979; Christensen, 1990), and the Mori-Tanaka method (Mori and Tanaka, 1973; Taya and Mura, 1981; Taya, 1981; Weng, 1984, 1990; Qiu and Weng, 1990). Nevertheless, effective medium methods do not depend on particle locations or their relative configurations. By contrast, the third school aims at *direct* micromechanics determination of effective properties of composites with *randomly located* and *interacting* inclusions by employing some approximations, or with certain special geometric configurations for inclusions dispersing in matrix materials. For example, the second-order formulations with pairwise inter-particle interactions were proposed in the 1970s for perfectly randomly dispersed spherical particles. Further, a micromechanical higher-order ensemble-volume average formulation was proposed by Ju and Chen (1994a, 1994b) for isotropically randomly located spherical particles. For aligned fiber reinforced composites, however, no such work was proposed along the line of the third school. Only *local* (not overall) plane-strain fiber interactions were investigated in the literature; see, e.g., Shioya (1971), Kouris and Tsuchida (1991), Honein (1991), and Honein et al. (1992, 1994a, 1994b).

In this paper, we attempt to construct an approximate yet accurate method to account for inter-fiber interaction effects in fiber reinforced composites. In combination with the ensemble-area averaged field equations, this work presents a new, higher-order (in fiber volume fraction ϕ), probabilistic approach to estimate effective transverse elastic moduli of two-phase composites containing unidirectionally aligned yet randomly located circular fibers.

This paper is organized as follows. In Section 2, approximate solutions for the local interaction problem of two identical yet randomly located elastic circular fibers embedded in an elastic matrix are presented. Subsequently, the ensemble-area averaged eigenstrain is obtained through probabilistic pairwise fiber interaction mechanism in Section 3. Both uniform and general radial distribution functions are considered. Combining the results from Sections 2–3 and the governing ensemble-area averaged field equations, effective transversely isotropic elastic moduli of fiber reinforced composites are derived in Section 4. It is found that our "noninteracting solutions" (obtained by dropping the pairwise fiber interactions) are *identical* to the variational bounds of Hashin (1965). In addition, comparisons and simulations between our predictions and other methods as well as experimental data are given in Section 5. By the analogy between the effective transverse shear modulus and the effective transverse shear viscosity, we extend our predictions to fiber suspensions with rigid fibers and an incompressible viscous fluid matrix.

2. APPROXIMATE LOCAL SOLUTIONS OF TWO INTERACTING CIRCULAR FIBERS

Shioya (1971) proposed an analysis for an infinitely large, thin plate containing a pair of circular elastic inhomogeneities and subjected to uniform tensions. Shioya's method was based on the Airy's stress function in the generalized plane stress and employed the bipolar coordinates together with a method of perturbation. Kouris and Tsuchida (1991) presented an analytical method to solve the elastic interaction problem between two circular fibers under the plane strain thermal loading. Their method was based on the displacement potential approach. Furthermore, Honein (1991, Chp. 7) and Honein *et al.* (1994a, 1994b) proposed a general framework to solve the problem of two circular inclusions in plane elastostatics, subject to arbitrary loading. Honein's approach hinged on the use of the Kolosov-Muskhelishvili complex potentials. Although the aforementioned methods are valuable, they are computationally involved and require numerical calculations of many terms in some infinite series.

In this section, instead of trying to derive exact local solutions of the randomly located two circular fibers interaction problem, we attempt to construct simple and accurate approximate analytical solutions. The proposed local approximate analytical solutions are quite compact and amenable to the pairwise ensemble-area average approach (to be explained in Section 3), leading to accurate estimates of effective elastic transverse moduli of two-phase composites containing many randomly located yet unidirectionally aligned circular fibers at moderately high volume fractions. For mathematical simplicity, we will assume that circular fibers are of equal size in what follows.

Let us consider two identical, unidirectionally aligned elastic circular fibers (phase 1) of radius a embedded in a homogeneous elastic matrix (phase 0). Since plane strain is assumed, the inclusion interaction exists only in the same cutting plane as shown in Fig. 2. In addition, the plane-strain linearly elastic isotropic stiffness tensors for both phases are denoted by

$$(\mathbf{C}_\alpha)_{ijkl} = \lambda_\alpha \delta_{ij}\delta_{kl} + \mu_\alpha(\delta_{ik}\delta_{jl} + \delta_{il}\delta_{jk}), \quad \alpha = 0, 1\,; i, j, k, l = 1, 2 \tag{1}$$

where λ_α and μ_α are the Lamé constants of the phase α material.

Following the eigenstrain concept introduced by Eshelby (1957), an integral equation governing the distributed eigenstrain $\boldsymbol{\varepsilon}^*(\mathbf{x})$ for a given particle (fiber) configuration and remote strain field $\boldsymbol{\varepsilon}^0$ was derived in eqn (7) in Ju and Chen (1994a). Within the present two-fiber context, the integral equation can be rephrased as follows:

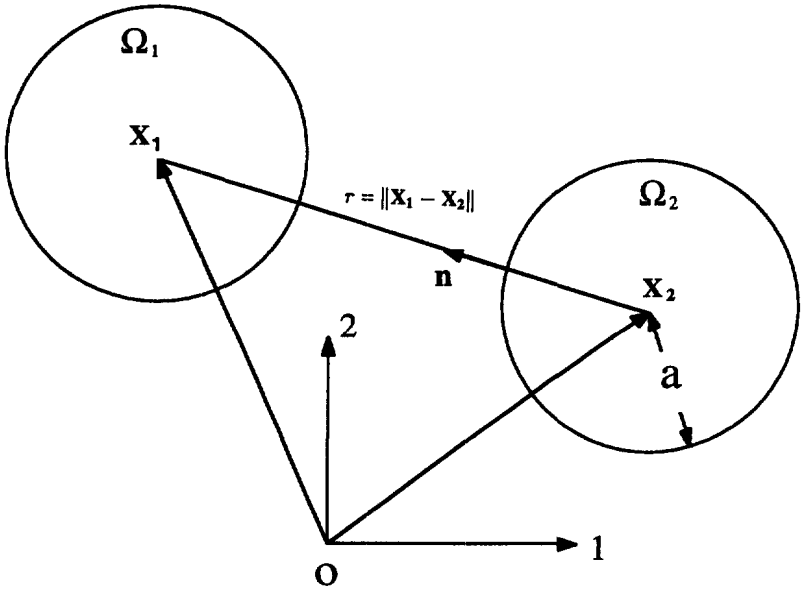

Fig. 2. Schematic diagram for the plane-strain two-fiber interaction problem.

$$-\mathbf{A}:\boldsymbol{\varepsilon}^{*(i)}(\mathbf{x}) = \boldsymbol{\varepsilon}^{o} + \int_{\Omega_i} \mathbf{G}(\mathbf{x}-\mathbf{x}'):\boldsymbol{\varepsilon}^{*(i)}(\mathbf{x}')\,d\mathbf{x}' + \int_{\Omega_j} \mathbf{G}(\mathbf{x}-\mathbf{x}'):\boldsymbol{\varepsilon}^{*(j)}(\mathbf{x}')\,d\mathbf{x}', \quad i \neq j, i,j = 1,2 \tag{2}$$

where $\mathbf{x} \in \Omega_i$ and $\boldsymbol{\varepsilon}^{*(i)}(\mathbf{x})$ is the eigenstrain at $\mathbf{x}$ in the i-th fiber domain Ω_i. In addition, the fourth-rank tensor $\mathbf{A}$ is defined as

$$\mathbf{A} \equiv (\mathbf{C}_1 - \mathbf{C}_0)^{-1} \cdot \mathbf{C}_0 \tag{3}$$

and the components of the fourth-rank two-dimensional Green's function tensor $\mathbf{G}$ are given by ($i,j,k,l = 1,2$; Mura, 1987):

$$G_{ijkl}(\mathbf{x}-\mathbf{x}') = \frac{1}{4\pi(1-\nu_0)r'^2} F_{ijkl}(-8, 2\nu_0, 2, 2-4\nu_0, -1+2\nu_0, 1-2\nu_0) \tag{4}$$

where $\mathbf{r}' \equiv \mathbf{x}-\mathbf{x}'$ and $r' \equiv \|\mathbf{r}'\|$. The components of the fourth-rank tensor $\mathbf{F}$—which depends on its arguments ($B_1, B_2, B_3, B_4, B_5, B_6$)—are defined by ($m$ = 1–6):

$$\begin{aligned} F_{ijkl}(B_m) \equiv\ & B_1 n'_i n'_j n'_k n'_l + B_2(\delta_{ik} n'_j n'_l + \delta_{il} n'_j n'_k + \delta_{jk} n'_i n'_l + \delta_{jl} n'_i n'_k) \\ & + B_3 \delta_{ij} n'_k n'_l + B_4 \delta_{kl} n'_i n'_j + B_5 \delta_{ij}\delta_{kl} + B_6(\delta_{ik}\delta_{jl} + \delta_{il}\delta_{jk}) \end{aligned} \tag{5}$$

with the normal vector $\mathbf{n}' \equiv \mathbf{r}'/r'$. All physical quantities refer to the Cartesian coordinates, and the summation convention applies. Moreover, δ_{ij} denotes the Kronecker delta and ν_0 is the Poisson's ratio of the matrix material.

As indicated in Ju and Chen (1994a, 1994b), the "noninteracting" solution for the eigenstrain, denoted by $\boldsymbol{\varepsilon}^{*o}$, can be obtained by neglecting the last term in the right-hand side of (2), which represents the interaction effect due to the other fiber. The "non-interacting" result is

$$-\mathbf{A}:\boldsymbol{\varepsilon}^{*o} = \boldsymbol{\varepsilon}^{o} + \mathbf{s}:\boldsymbol{\varepsilon}^{*o} \tag{6}$$

where the two-dimensional Eshelby tensor $\mathbf{s}$ is defined as

$$\mathbf{s} \equiv \int_{\Omega_i} \mathbf{G}(\mathbf{x}-\mathbf{x}')\,d\mathbf{x}';\ \mathbf{x},\mathbf{x}' \in \Omega_i \tag{7}$$

The components of $\mathbf{s}$ depend on the Poisson's ratio of the matrix (ν_0) and the shape of the fiber cross-sectional domain Ω_i. In particular, for a two-dimensional circular domain, the components of $\mathbf{s}$ are

$$s_{ijkl} = \frac{1}{8(1-\nu_0)}\{(4\nu_0-1)\delta_{ij}\delta_{kl} + (3-4\nu_0)(\delta_{ik}\delta_{jl}+\delta_{il}\delta_{jk})\}. \tag{8}$$

See Mura (1987) and Appendix A for more details.

By subtracting the noninteracting solution (6) from (2), the effect of inter-fiber interaction can be found by solving the following integral equation:

$$-\mathbf{A}:\mathbf{d}^{*(i)}(\mathbf{x}) = \int_{\Omega_j} \mathbf{G}(\mathbf{x}-\mathbf{x}')\,d\mathbf{x}':\boldsymbol{\varepsilon}^{*o} + \int_{\Omega_i} \mathbf{G}(\mathbf{x}-\mathbf{x}'):\mathbf{d}^{*(i)}(\mathbf{x}')\,d\mathbf{x}' + \int_{\Omega_j} \mathbf{G}(\mathbf{x}-\mathbf{x}'):\mathbf{d}^{*(j)}(\mathbf{x}')\,d\mathbf{x}', \quad \text{for } \mathbf{x}\in\Omega_i, \quad i\neq j \tag{9}$$

where

$$\mathbf{d}^{*(i)}(\mathbf{x}) \equiv \boldsymbol{\varepsilon}^{*(i)}(\mathbf{x}) - \boldsymbol{\varepsilon}^{*o}. \tag{10}$$

To obtain the higher-order interaction correction for $\boldsymbol{\varepsilon}^{*(i)}(\mathbf{x})$, one may expand the fourth-rank tensor $\mathbf{G}(\mathbf{x}-\mathbf{x}')$ in the domain Ω_j with respect to its central point $\mathbf{x}_j$; i.e.,

$$\mathbf{G}(\mathbf{x}-\mathbf{x}') = \mathbf{G}(\mathbf{x}-\mathbf{x}_j) - (\mathbf{x}'-\mathbf{x}_j)\cdot[\nabla_{\mathbf{x}}\otimes\mathbf{G}(\mathbf{x}-\mathbf{x}_j)] + \tfrac{1}{2}[(\mathbf{x}'-\mathbf{x}_j)\otimes(\mathbf{x}'-\mathbf{x}_j)]:[\nabla_{\mathbf{x}}\otimes\nabla_{\mathbf{x}}\otimes\mathbf{G}(\mathbf{x}-\mathbf{x}_j)] + \cdots \tag{11}$$

in which the relation

$$\nabla_{\mathbf{x}'}\otimes\mathbf{G}(\mathbf{x}-\mathbf{x}') = -\nabla_{\mathbf{x}}\otimes\mathbf{G}(\mathbf{x}-\mathbf{x}') \tag{12}$$

has been used. From eqns (9) and (11), we have

$$-\mathbf{A}:\mathbf{d}^{*(i)}(\mathbf{x}) = \int_{\Omega_j} \mathbf{G}(\mathbf{x}-\mathbf{x}')\,d\mathbf{x}':\boldsymbol{\varepsilon}^{*o} + \int_{\Omega_i} \mathbf{G}(\mathbf{x}-\mathbf{x}'):\mathbf{d}^{*(i)}(\mathbf{x}')\,d\mathbf{x}' + \Omega\mathbf{G}(\mathbf{x}-\mathbf{x}_j):\bar{\mathbf{d}}^{*(j)}(\mathbf{x}_j) - \Omega a\{\nabla_{\mathbf{x}}\otimes\mathbf{G}(\mathbf{x}-\mathbf{x}_j)\}:\bar{\mathbf{P}}^{*(j)} + \frac{1}{2}\Omega a^2\{\nabla_{\mathbf{x}}\otimes\nabla_{\mathbf{x}}\otimes\mathbf{G}(\mathbf{x}-\mathbf{x}_j)\}:\bar{\mathbf{Q}}^{*(j)} + \cdots \tag{13}$$

for $\mathbf{x}\in\Omega_i$ and $i\neq j$ $(i,j=1,2)$. Here, $\Omega=\pi a^2$ is the cross-sectional area of a single fiber, and a is its radius. Furthermore, the average fields involved in (13) are defined as follows

$$\bar{\mathbf{d}}^{*(j)} \equiv \frac{1}{\Omega}\int_{\Omega_j} \mathbf{d}^{*(j)}(\mathbf{x})\,d\mathbf{x} \tag{14}$$

$$\bar{\mathbf{P}}^{*(j)} \equiv \frac{1}{\Omega a}\int_{\Omega_j} (\mathbf{x}-\mathbf{x}_j)\otimes\mathbf{d}^{*(j)}(\mathbf{x})\,d\mathbf{x} \tag{15}$$

$$\bar{\mathbf{Q}}^{*(j)} \equiv \frac{1}{\Omega a^2}\int_{\Omega_j} (\mathbf{x}-\mathbf{x}_j)\otimes(\mathbf{x}-\mathbf{x}_j)\otimes \mathbf{d}^{*(j)}(\mathbf{x})\,d\mathbf{x}. \tag{16}$$

The third rank tensor $\bar{\mathbf{P}}^{*(j)}$ and the fourth rank tensor $\bar{\mathbf{Q}}^{*(j)}$ correspond to the dipole and quadrapole of $\mathbf{d}^{*(i)}$ in the domain Ω_j, respectively. Due to the circular symmetry of fibers, the leading order of $\bar{\mathbf{P}}^{*(i)}$ can be shown to be of the order $O(\rho^3)$, rather than $O(\rho^2)$, by substituting (13) into (15). Here, $\rho \equiv a/r$ and r is the spacing between the centers of two interacting fibers. By performing the *area average* of (13) for the domain Ω_i and neglecting those terms of higher order moments in (13), the *approximate* equations for $\bar{\mathbf{d}}^{*(i)}$ for the two-fiber interaction problem can be obtained:

$$-\mathbf{A}:\bar{\mathbf{d}}^{*(i)} = \mathbf{G}^2(\mathbf{x}_i-\mathbf{x}_j):\boldsymbol{\varepsilon}^{*o}+\mathbf{s}:\bar{\mathbf{d}}^{*(i)}+\mathbf{G}^1(\mathbf{x}_i-\mathbf{x}_j):\bar{\mathbf{d}}^{*(j)}+O(\rho^6) \tag{17}$$

where

$$\mathbf{G}^1 \equiv \int_{\Omega_1}\mathbf{G}(\mathbf{x}-\mathbf{x}_2)\,d\mathbf{x} = \int_{\Omega_2}\mathbf{G}(\mathbf{x}_1-\mathbf{x})\,d\mathbf{x} = \frac{1}{8(1-\nu_0)}\left(\rho^2\mathbf{H}^1+\frac{\rho^4}{2}\mathbf{H}^2\right) \tag{18}$$

$$\mathbf{G}^2 \equiv \frac{1}{\Omega}\int_{\Omega_1}\int_{\Omega_2}\mathbf{G}(\mathbf{x}-\mathbf{x}')\,d\mathbf{x}'\,d\mathbf{x} = \frac{1}{8(1-\nu_0)}(\rho^2\mathbf{H}^1+\rho^4\mathbf{H}^2) \tag{19}$$

and the components of $\mathbf{H}^1$ and $\mathbf{H}^2$ are given by

$$H^1_{ijkl}(\mathbf{x}_1-\mathbf{x}_2) \equiv 2F_{ijkl}(-8, 2\nu_0, 2, 2-4\nu_0, -1+2\nu_0, 1-2\nu_0) \tag{20}$$

$$H^2_{ijkl}(\mathbf{x}_1-\mathbf{x}_2) \equiv 2F_{ijkl}(24, -4, -4, -4, 1, 1). \tag{21}$$

It is interesting to note that $\mathbf{G}^1$ in eqn (18) is *different* from the Eshelby tensor $\mathbf{s}$ defined in (7). One may refer to $\mathbf{G}^1$ as the "*exterior point* Eshelby tensor" since the integrals in (18) involves one *exterior point* (e.g., $\mathbf{x}_2$, the center of Ω_2) outside the integration domain (e.g., Ω_1).

It should be noted that the leading-order error induced by truncating the higher order moments in (17) is of the order $O(\rho^6)$, since both $\bar{\mathbf{P}}^{*(i)}$ and $\Omega a\nabla_{\mathbf{x}}\otimes\mathbf{G}$ are of the order $O(\rho^3)$. Furthermore, we observe from (17) that

$$\bar{\mathbf{d}}^{*(1)} = \bar{\mathbf{d}}^{*(2)} \equiv \bar{\mathbf{d}}^{*}. \tag{22}$$

Therefore, the solutions of (17) are

$$\bar{\mathbf{d}}^{*} = -8(1-\nu_0)[\mathbf{T}^{-1}\cdot\mathbf{G}^2]:\boldsymbol{\varepsilon}^{*o}+O(\rho^6) \tag{23}$$

where

$$\mathbf{T}(\mathbf{x}_1-\mathbf{x}_2) \equiv -8(1-\nu_0)\{-\mathbf{A}-\mathbf{s}-\mathbf{G}^1(\mathbf{x}_1-\mathbf{x}_2)\}. \tag{24}$$

The procedure for finding the inverse of the fourth-rank tensor $\mathbf{T}$ is given in Appendix B. The corresponding expression to the order of $O(\rho^2)$ is

$$\mathbf{T}^{-1} = \mathbf{K}^{-1}+\rho^2\mathbf{L}+O(\rho^4) \tag{25}$$

where

$$K_{ijkl} \equiv F_{ijkl}(0, 0, 0, 0, \alpha, \beta) \tag{26}$$

$$L_{ijkl} \equiv \frac{1}{\beta^2} F_{ijkl}\left(4, -\nu_0, -2(1-\nu_0)+\frac{\beta(1-2\nu_0)}{\alpha+\beta}, -2(1-\nu_0)+\frac{\beta}{\alpha+\beta}, \frac{3-4\nu_0}{2}-\frac{\beta(1-\nu_0)}{\alpha+\beta}, -\frac{1-2\nu_0}{2}\right) \tag{27}$$

and

$$\alpha = (4\nu_0 - 1) + 4(1-\nu_0)\cdot\left(\frac{\kappa_0}{\kappa_1-\kappa_0} - \frac{\mu_0}{\mu_1-\mu_0}\right) \tag{28}$$

$$\beta = (3-4\nu_0) + 4(1-\nu_0)\frac{\mu_0}{\mu_1-\mu_0}. \tag{29}$$

Here, κ_0, κ_1 and μ_0, μ_1 are the plane strain bulk and shear moduli of the matrix and fiber phases, respectively. Substitution of (25) into (23) then renders the final expression for $\bar{\mathbf{d}}^*$.

$$\bar{\mathbf{d}}^* = -[\mathbf{K}^{-1}\cdot(\rho^2\mathbf{H}^1 + \rho^4\mathbf{H}^2)] : \boldsymbol{\varepsilon}^{*o} - \rho^4[\mathbf{L}\cdot\mathbf{H}^1] : \boldsymbol{\varepsilon}^{*o} + O(\rho^6) \tag{30}$$

Since $r > 2a$, we have $\rho < \frac{1}{2}$.

3. ENSEMBLE-AREA AVERAGED EIGENSTRAINS

In order to obtain the ensemble-average solution of $\bar{\mathbf{d}}^*$ within the context of approximate pair-wise fiber interaction, one has to integrate (30) over all possible positions ($\mathbf{x}_2$) of the second fiber for a given location of the first fiber ($\mathbf{x}_1$). The ensemble-average process can be written as

$$\langle\bar{\mathbf{d}}^*\rangle(\mathbf{x}_1) = \int_{A-\Omega_1} \bar{\mathbf{d}}^*(\mathbf{x}_1 - \mathbf{x}_2) P(\mathbf{x}_2|\mathbf{x}_1)\, d\mathbf{x}_2 \tag{31}$$

where $P(\mathbf{x}_2|\mathbf{x}_1)$ is the conditional probability function for finding the second fiber centered at $\mathbf{x}_2$ given the first fiber centered at $\mathbf{x}_1$. Moreover, angled brackets signify the ensemble (probabilistic) average operators. In this paper, we shall consider only two-dimensional, statistically transversely *isotropic* and homogeneous two-point probability function $P(\mathbf{x}_2|\mathbf{x}_1)$. The (infinitely large) 2-D transversely isotropic *probabilistic* (not physical) integration domain A in (31) can therefore be evaluated as circular. It is noted that Ω_1 in (31) defines the probabilistic "exclusion zone" for $\mathbf{x}_2$.

The two-point conditional probability function $P(\mathbf{x}_2|\mathbf{x}_1)$ depends on the 2-D *microstructure* of a composite which in turn depends on the fiber volume fraction and the underlying manufacturing processes. In the absence of actual manufacturing and microstructural evidences, it is often assumed that the 2-D point conditional probability function takes the following form:

$$P(\mathbf{x}_2|\mathbf{x}_1) = \begin{cases} \dfrac{N}{A} g(\hat{r}), & \text{if } \hat{r} \geqslant 1 \\ 0, & \text{otherwise} \end{cases} \tag{32}$$

where N/A is the 2-D number density of fibers in a composite and r is the spacing between the centers of two fibers ($\hat{r} \equiv r/2a$). Further, $g(\hat{r})$ denotes the 2-D transversely isotropic "radial distribution function".

Case I: *Uniform radial distribution function*

In this case, we have $g(\hat{r}) = 1$. This corresponds to the simplest approximation for $g(\hat{r})$ since it tends to underestimate the probability of the second fiber ($\mathbf{x}_2$) in the near neighborhood of the first fiber ($\mathbf{x}_1$) at high fiber volume fraction. Therefore, this case may be regarded as the "lower bound" for microstructure and is more suitable for low fiber concentrations. By substituting eqn (30) and (32) into eqn (31), the explicit expression for $\langle \bar{\mathbf{d}}^* \rangle(\mathbf{x}_1)$ can be rephrased as

$$\langle \bar{\mathbf{d}}^* \rangle(\mathbf{x}_1) = -\frac{N}{A}\mathbf{K}^{-1} : \left\{ \int_{2a}^{\infty} \rho^2 r \int_0^{2\pi} \mathbf{H}^1(\mathbf{n})\, \mathrm{d}\theta\, \mathrm{d}r + \int_{2a}^{\infty} \rho^4 r \int_0^{2\pi} \mathbf{H}^2(\mathbf{n})\, \mathrm{d}\theta\, \mathrm{d}r \right\} : \boldsymbol{\varepsilon}^{*o}$$
$$- \frac{N}{A}\left\{ \int_{2a}^{\infty} \rho^4 r \int_0^{2\pi} [\mathbf{L}(\mathbf{n}) \cdot \mathbf{H}^1(\mathbf{n})]\, \mathrm{d}\theta\, \mathrm{d}r \right\} : \boldsymbol{\varepsilon}^{*o} + \cdots \tag{33}$$

where $\mathbf{n}$ is the normal vector (i.e., $\mathbf{n} = \mathbf{r}/r$ with $\mathbf{r} = \mathbf{x}_2 - \mathbf{x}_1$). In addition, the following identities can be easily derived:

$$\int_0^{2\pi} n_i n_j \, \mathrm{d}\theta = \pi \delta_{ij} \tag{34}$$

$$\int_0^{2\pi} n_i n_j n_k n_l \, \mathrm{d}\theta = \frac{\pi}{4}(\delta_{ij}\delta_{kl} + \delta_{ik}\delta_{jl} + \delta_{il}\delta_{jk}). \tag{35}$$

It is straightforward to verify that the integrals of $\mathbf{H}^1$ and $\mathbf{H}^2$ in the first line of (33) are *identically zero*.

The (approximate) ensemble-area averaged eigenstrain tensor can now be obtained by substituting the expression for $\mathbf{L}$ and $\mathbf{H}^1$ into the integral of (33) and utilizing the identities (34)–(35), together with the definition of $\bar{\mathbf{d}}^{*(i)}$ in (14). The final expression (based on (32)) reads:

$$\langle \boldsymbol{\varepsilon}^* \rangle = \boldsymbol{\Gamma} : \boldsymbol{\varepsilon}^{*o} \tag{36}$$

where the components of the *isotropic* tensor $\boldsymbol{\Gamma}$ are rendered by

$$\Gamma_{ijkl} = \gamma_1 \delta_{ij}\delta_{kl} + \gamma_2(\delta_{ik}\delta_{jl} + \delta_{il}\delta_{jk}) \tag{37}$$

in which

$$\gamma_1 = \frac{\phi}{4\beta^2}\left[-2 + \frac{\beta(1-2\nu_0)}{\alpha+\beta} \right] \tag{38}$$

$$\gamma_2 = \frac{1}{2} + \frac{\phi}{4\beta^2}\left[2 + \frac{\beta(1-2\nu_0)}{\alpha+\beta} \right]. \tag{39}$$

It is noticed that, in deriving (36), the ensemble average $\langle \bar{\mathbf{d}}^* \rangle(\mathbf{x}_i)$ is a *constant* for any particle centered at $\mathbf{x}_i$—a consequence of (22) or (17). Clearly, eqn (36) is a truly *closed-form* analytical formula.

Case II: *General radial distribution function*

For a general 2-D transversely isotropic radial distribution function $g(r)$ (which depends on the fiber volume fraction ϕ), the ensemble integration of (30) leads to

$$\langle \bar{\mathbf{d}}^* \rangle = \frac{N}{A} \int_{2a}^{\infty} r g(r) \left[\int_0^{2\pi} \bar{\mathbf{d}}^* \, \mathrm{d}\theta \right] \mathrm{d}r \tag{40}$$

or

$$\langle \bar{\mathbf{d}}^* \rangle = \frac{N}{A} \frac{2\pi}{\beta^2} \mathbf{W} : \boldsymbol{\varepsilon}^{*o} \times \int_{2a}^{\infty} \frac{a^4}{r^3} g(r) \, \mathrm{d}r \tag{41}$$

where

$$W_{ijkl} \equiv \xi_1 \delta_{ij} \delta_{kl} + \xi_2 (\delta_{ik} \delta_{jl} + \delta_{il} \delta_{jk}) \tag{42}$$

$$\xi_1 = -2 + \frac{\beta(1 - 2\nu_0)}{\alpha + \beta} \tag{43}$$

$$\xi_2 = 2 + \frac{\beta(1 - 2\nu_0)}{\alpha + \beta}. \tag{44}$$

Furthermore, we have

$$\int_{2a}^{\infty} \frac{a^4}{r^3} g(r) \, \mathrm{d}r = a^2 \int_0^{\frac{1}{2}} \rho g(\rho) \, \mathrm{d}\rho \equiv a^2 Y(g). \tag{45}$$

Therefore, $\langle \bar{\mathbf{d}}^* \rangle$ and $\boldsymbol{\Gamma}$ can be rephrased, respectively, as

$$\langle \bar{\mathbf{d}}^* \rangle = \frac{2\phi}{\beta^2} Y(g) \mathbf{W} : \boldsymbol{\varepsilon}^{*o} \tag{46}$$

$$\boldsymbol{\Gamma} = \mathbf{I} + \frac{2\phi}{\beta^2} Y(g) \mathbf{W} \equiv \gamma_1(g) \mathbf{1} \otimes \mathbf{1} + 2\gamma_2(g) \mathbf{I} \tag{47}$$

where

$$\gamma_1(g) = \frac{2\phi}{\beta^2} Y(g) \left[-2 + \frac{\beta(1 - 2\nu_0)}{\alpha + \beta} \right] \tag{48}$$

$$\gamma_2(g) = \frac{1}{2} + \frac{2\phi}{\beta^2} Y(g) \left[2 + \frac{\beta(1 - 2\nu_0)}{\alpha + \beta} \right]. \tag{49}$$

Consequently, the "interaction-effect tensor" $\boldsymbol{\Gamma}$ can be explicitly computed for any 2-D transversely isotropic radial distribution function at any specified fiber volume fraction ϕ.

For example, at higher fiber volume fractions, it is sometimes assumed that the two-point conditional probability function obeys the so-called thermodynamic "equilibrium radial distribution function" (ERDF) as follows:

$$g(\hat{r}) = H(\hat{r} - 1)[1 + A(\hat{r})\phi] \tag{50}$$

where (recalling that $\hat{r} \equiv r/2a$; Hansen and McDonald (1986), Torquato and Lado (1992))

$$A(\hat{r}) = \frac{4}{\pi} \left[\pi - 2 \sin^{-1} \left(\frac{\hat{r}}{2} \right) - \hat{r} \left(1 - \frac{\hat{r}^2}{4} \right)^{1/2} \right] H(2 - \hat{r}) \tag{51}$$

$$H(x) = \begin{cases} 0, & x \leqslant 0 \\ 1, & x > 0. \end{cases} \tag{52}$$

The integration in eqn (45) for this ERDF case can be easily obtained by numerical calculation:

$$Y(g) \equiv \int_0^{1/2} \rho g(\rho)\, \mathrm{d}\rho = \frac{1}{8} + 0.0865\phi. \tag{53}$$

On the other hand, for a statistically uniform radial distribution function, we have $g = 1$ and thus $Y = 1/8$. Therefore, Case I is easily recovered.

4. EFFECTIVE TRANSVERSE ELASTIC MODULI OF TWO-PHASE COMPOSITES CONTAINING UNIDIRECTIONALY ALIGNED CIRCULAR FIBERS

We now focus on the derivation of effective transverse elastic moduli of composites containing randomly located, unidirectionally aligned circular fibers. We shall employ the pairwise interaction solutions for $\langle \bar{\boldsymbol{\varepsilon}}^* \rangle$ (from Section 3) and other ensemble-area averaged field equations. The proposed procedure can be readily modified to include circular fibers of different sizes and/or elastic properties. In what follows, angle brackets denoting the ensemble-average operators will be dropped for simplicity.

In accord with Ju and Chen (1994a) and Zhao *et al.* (1989), we have the following relations governing the averaged stress ($\bar{\boldsymbol{\sigma}}$), the averaged strain ($\bar{\boldsymbol{\varepsilon}}$), the uniform remote strain ($\boldsymbol{\varepsilon}^o$) and the averaged eigenstrain ($\bar{\boldsymbol{\varepsilon}}^*$):

$$\bar{\boldsymbol{\sigma}} = \mathbf{C}_0 : (\bar{\boldsymbol{\varepsilon}} - \phi \bar{\boldsymbol{\varepsilon}}^*) \tag{54}$$

$$\bar{\boldsymbol{\varepsilon}} = \boldsymbol{\varepsilon}^o + \phi \mathbf{s} : \bar{\boldsymbol{\varepsilon}}^*. \tag{55}$$

Upon substitution of the solution of $\bar{\boldsymbol{\varepsilon}}^*$ in (36) or (47) into (55) and utilizing the relation between $\boldsymbol{\varepsilon}^o$ and $\boldsymbol{\varepsilon}^{*o}$ given by (6), the relation between the averaged eigenstrain $\bar{\boldsymbol{\varepsilon}}^*$ and the averaged strain $\bar{\boldsymbol{\varepsilon}}$ is expressed as

$$\bar{\boldsymbol{\varepsilon}}^* = [\boldsymbol{\Gamma} \cdot (-\mathbf{A} - \mathbf{s} + \phi \mathbf{s} \cdot \boldsymbol{\Gamma})^{-1}] : \bar{\boldsymbol{\varepsilon}}. \tag{56}$$

The above expression is valid for any 2-D transversely isotropic radial distribution function $g(r)$.

Moreover, substitution of (56) into (54) renders the effective stiffness $\mathbf{C}^*$ relating $\bar{\boldsymbol{\sigma}}$ and $\bar{\boldsymbol{\varepsilon}}$:

$$\mathbf{C}^* = \mathbf{C}_0 \cdot \{\mathbf{I} - \phi \boldsymbol{\Gamma} \cdot (-\mathbf{A} - \mathbf{s} + \phi \mathbf{s} \cdot \boldsymbol{\Gamma})^{-1}\}. \tag{57}$$

Since all the fourth-rank tensors on the right-hand side of (57) are isotropic in two-dimension, the effective stiffness tensor $\mathbf{C}^*$ for this two-phase composite is also *isotropic* in 2-D (or, equivalently transversely isotropic in three-dimension). Accordingly, the effective *plane-strain* bulk modulus κ^* and shear modulus μ_T^* can be explicitly evaluated:

$$\kappa^* = \kappa_0 \left\{ 1 + \frac{8\phi(1-\nu_0)(\gamma_1+\gamma_2)}{(\alpha+\beta) - 4\phi(\gamma_1+\gamma_2)} \right\} \tag{58}$$

$$\mu_T^* = \mu_0 \left\{ 1 + \frac{8\phi(1-\nu_0)\gamma_2}{\beta - 2(3-4\nu_0)\phi\gamma_2} \right\}. \tag{59}$$

It should be noted that the definition of the effective plane-strain bulk modulus is $\kappa^2 \equiv \lambda^* + \mu_T^*$, where λ^* and μ_T^* are the effective Lamé constants. In addition, γ_1 and γ_2 are previously defined by (48)–(49). In particular, we have

$$Y(g) = \begin{cases} \frac{1}{8}, & \text{for uniform radial distribution} \\ \frac{1}{8}+0.0865\phi, & \text{for equilibrium radial distribution} \end{cases}. \tag{60}$$

We shall now consider some interesting special cases.

Case I: Noninteracting solution. If near-field pairwise fiber interactions are totally neglected, we obtain the so-called "noninteracting" approximation for effective transverse elastic properties. The noninteracting solution can be easily acquired by dropping the pairwise interaction effects; i.e., let $\mathbf{\Gamma} = \mathbf{I}$ with $\gamma_1 = 0$ and $\gamma_2 = 1/2$. Accordingly, the plane-strain effective bulk modulus κ^* and transverse shear modulus μ_T^* reduce to:

$$\kappa^* = \kappa_0 \left\{ 1 + \frac{\phi}{\dfrac{\kappa_0}{\kappa_1 - \kappa_0} + (1-\phi)\dfrac{\kappa_0}{\kappa_0 + \mu_0}} \right\} \tag{61}$$

$$\mu_T^* = \mu_0 \left\{ 1 + \frac{\phi}{\dfrac{\mu_0}{\mu_1 - \mu_0} + (1-\phi)\dfrac{\kappa_0 + 2\mu_0}{2(\kappa_0 + \mu_0)}} \right\}. \tag{62}$$

It is observed that these "noninteracting" expressions are *identical* to the variational lower bounds (4.25) and (4.27) of Hashin (1965); see also Hill (1964) for κ^* bounds.

Case II: Rigid fibers. For an *incompressible* elastic matrix containing randomly located and aligned identical *rigid* circular fibers, the proposed interacting solution renders the following effective transverse shear modulus:

$$\mu_T^* = \mu_0 \left\{ 1 + 2\phi \frac{1 + 8Y(g)\phi}{1 - \phi - 8Y(g)\phi^2} \right\}. \tag{63}$$

For the special cases of uniform and equilibrium radial distribution functions (RDFs), the singularity points in (63) occur at $\phi = 0.618$ and 0.562, respectively. Furthermore, the Taylor's series expansion of (63) with respect to ϕ renders

$$\mu_T^* = \mu_0 \{1 + 2\phi + 2[1 + 8Y(g)]\phi^2 + 2[1 + 16Y(g)]\phi^3 + O(\phi^4)\}. \tag{64}$$

Equation (64) reduces to

$$\mu_T^* = \mu_0 \{1 + 2\phi + 4\phi^2 + 6\phi^3 + O(\phi^4)\} \tag{65}$$

for the uniform RDF, and

$$\mu_T^* = \mu_0 \{1 + 2\phi + 4\phi^2 + 7.384\phi^3 + O(\phi^4)\} \tag{66}$$

for the equilibrium RDF. The coefficient for the $O(\phi)$ is 2 which is consistent with the dilute result of Eshelby (1957); see also Christensen (1993).

Case III: Cylindrical voids. For an *incompressible* matrix containing randomly located and aligned identical cylindrical voids, the proposed interacting solution leads to the following effective plane-strain bulk modulus and transverse shear modulus:

$$\kappa^* = \mu_0 \left\{ \frac{1}{4\phi^2 Y(g) + \phi} - 1 \right\} \tag{67}$$

$$\mu_T^* = \mu_0 \left\{ 1 - 2\phi \frac{1 + 10\phi Y(g)}{1 + \phi + 10\phi^2 Y(g)} \right\}. \tag{68}$$

5. SOME COMPARISONS AND SIMULATIONS

In order to illustrate the potential of the proposed micromechanical framework, we now compare our analytical predictions with Hill's (1964) and Hashin's (1965, 1972) two-point bounds, Silnutzer's (1972) three-point bounds (Milton (1982), Torquato and Lado (1992)), and limited available experimental data of Uemura *et al.* (1968). For demonstration purposes, we will consider the (statistically transversely isotropic) uniform and equilibrium RDFs. Following Kondo and Saito (1986), we will consider the following constituent elastic phase properties for the glass fiber reinforced epoxy matrix composite: $E_1 = 11{,}660$ kgf/mm^2, $\nu_1 = 0.22$ (glass fiber) and $E_0 = 550$ kgf/mm^2, $\nu_0 = 0.35$ (epoxy resin).

Figures 3 and 4 show the predicted plane-strain effective (normalized) bulk modulus κ^*/κ_0 and effective (normalized) transverse shear modulus μ_T^*/μ_0 of the glass-epoxy composites at various fiber volume fractions ϕ. We plot the theoretical predictions in Figs 3 and 4 based on Hashin's (1965) second-order bounds, Silnutzer's (1972) third-order bounds (with the equilibrium RDF following Torquato and Lado (1992)), and the proposed eqns (58)–(59) with the uniform and radial RDFs, respectively. Clearly, our analytical predictions are well within the Hashin's (1965) two-point bounds and Silnutzer's (1972) three-point bounds. We recall that our "non-interacting solutions" in the previous section

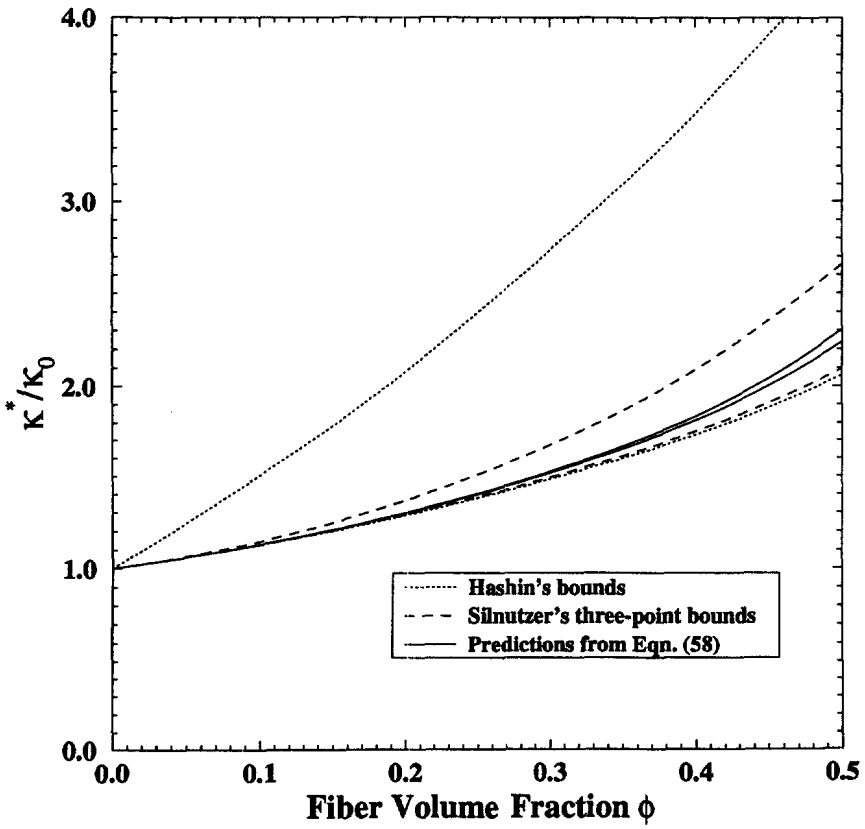

Fig. 3. The effective plane-strain bulk modulus vs. the fiber volume fraction ϕ. The upper and lower solid lines correspond to the present method with the equilibrium and the uniform RDFs, respectively.

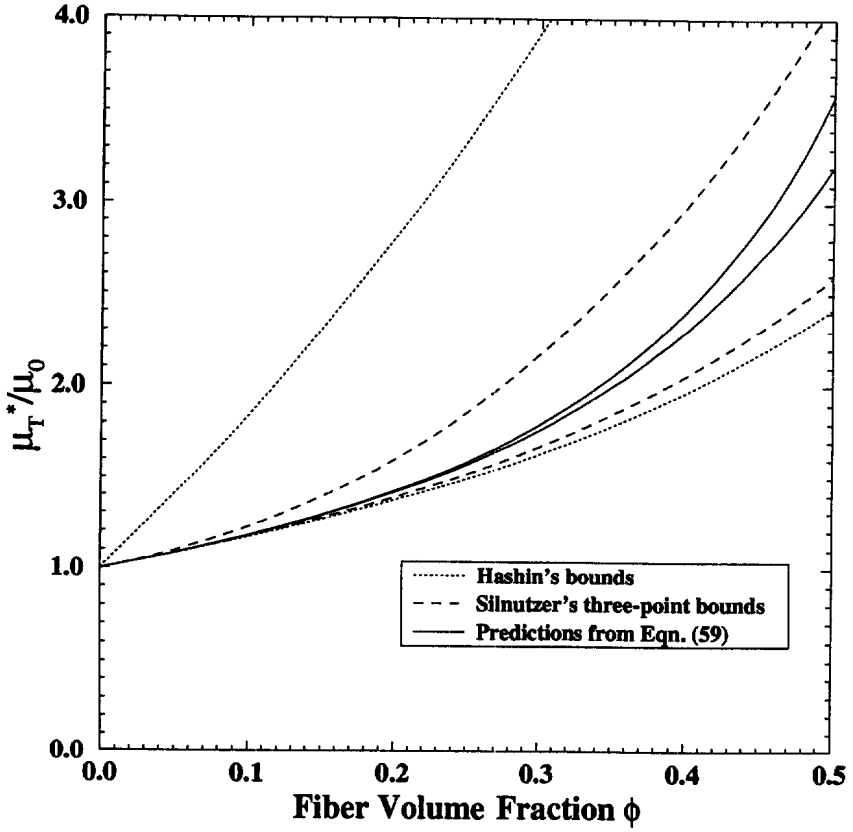

Fig. 4. The effective transverse shear modulus vs the fiber volume fraction ϕ. The upper and lower solid lines correspond to the present method with the equilibrium and uniform RDFs, respectively.

coincide precisely with Hashin's (1965) lower bounds for κ^* and μ_T^* of the reinforced elastic composites.

The proposed micromechanical *plane strain* framework cannot predict the effective axial (out-of-plane) Young's modulus E_A^* and effective axial Poisson's ratio ν_A^*. On the other hand, bounds on effective axial E_A^* and ν_A^* are available from Hashin (1972):

$$E_A^* = E_0\phi_0 + E_1\phi + \frac{4\phi\phi_0(\nu_1-\nu_0)^2}{\dfrac{\phi}{\kappa_0}+\dfrac{\phi_0}{\kappa_1}+\dfrac{1}{\mu_0}} \tag{69}$$

$$\nu_A^* = \nu_0\phi_0 + \nu_1\phi + \frac{\phi\phi_0(\nu_1-\nu_0)\left(\dfrac{1}{\kappa_0}-\dfrac{1}{\kappa_1}\right)}{\dfrac{\phi}{\kappa_0}+\dfrac{\phi_0}{\kappa_1}+\dfrac{1}{\mu_0}} \tag{70}$$

where $\phi_0 \equiv 1-\phi$. According to the calculations of Kondo and Saito (1986) and the present authors, eqns (69) and (70) render highly accurate predictions because the lower and upper bounds of Hashin (1972) are extremely close to each other. Even the simple mixture rule (the first two terms on the right-hand side of (69)–(70)) provides fairly good estimates for effective axial E_A^* and ν_A^*. Therefore, the out-of-plane fiber interaction effects are insignificant as far as E_A^* and ν_A^* are concerned.

Consequently, the effective *transverse* Young's modulus E_T^* and Poisson's ratio ν_T^* can be predicted by combining our eqns (58)–(59) for κ^* and μ_T^* and (69)–(70) for E_A^* and ν_A^*:

$$E_T^* = \frac{4\kappa^*\mu_T^*}{\kappa^* + \psi\mu_T^*} \tag{71}$$

$$\nu_T^* = \frac{\kappa^* - \psi\mu_T^*}{\kappa^* + \mu_T^*} \tag{72}$$

where

$$\psi = 1 + \frac{4\nu_A^{*2}\kappa^*}{E_A^*}. \tag{73}$$

The above expressions were given by Hashin and Rosen (1964); see eqns (17)–(18) therein. Figure 5 depicts the predictions for the effective transverse Young's modulus E_T^* according to the proposed eqn (58)–(59) and (71), and the Hashin's (1972) bounds. Both the uniform and equilibrium RDFs are employed to illustrate the proposed model. In addition, the experimental data of Uemura *et al.* (1968) for the glass-epoxy composites are plotted in Figure 5 for comparison purpose. It is observed that the proposed formulation compares very well with experimental data for ϕ up to about 55%. For fiber volume fraction ϕ greater than 60%, micro-defects may exist widely in experimental specimens. Therefore, interface debonding as well as fracture may significantly affect the overall mechanical behavior of composites at very dense fibre concentrations. Furthermore, higher-order fiber interactions would need to be considered for $\phi \geqslant 60\%$ by means of rigorous micro-mechanics and the ensemble-area averaging procedure.

It is also interesting to illustrate the potential of the proposed method in predicting the effective elastic moduli of brittle elastic matrix containing randomly located yet unidirectionally aligned cylindrical *voids*. In such event, we simply have $\kappa_0 = 0$ and $\mu_1 = 0$ for

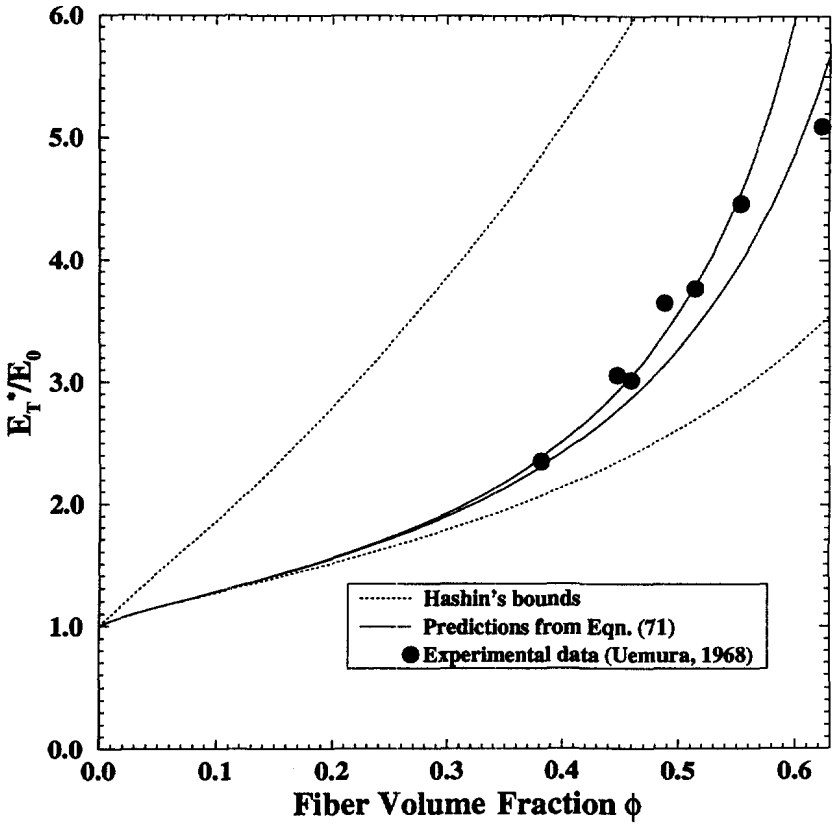

Fig. 5. The effective transverse Young's modulus vs the fiber volume fraction ϕ. The upper and lower solid lines correspond to the present method with the equilibrium and uniform RDFs, respectively.

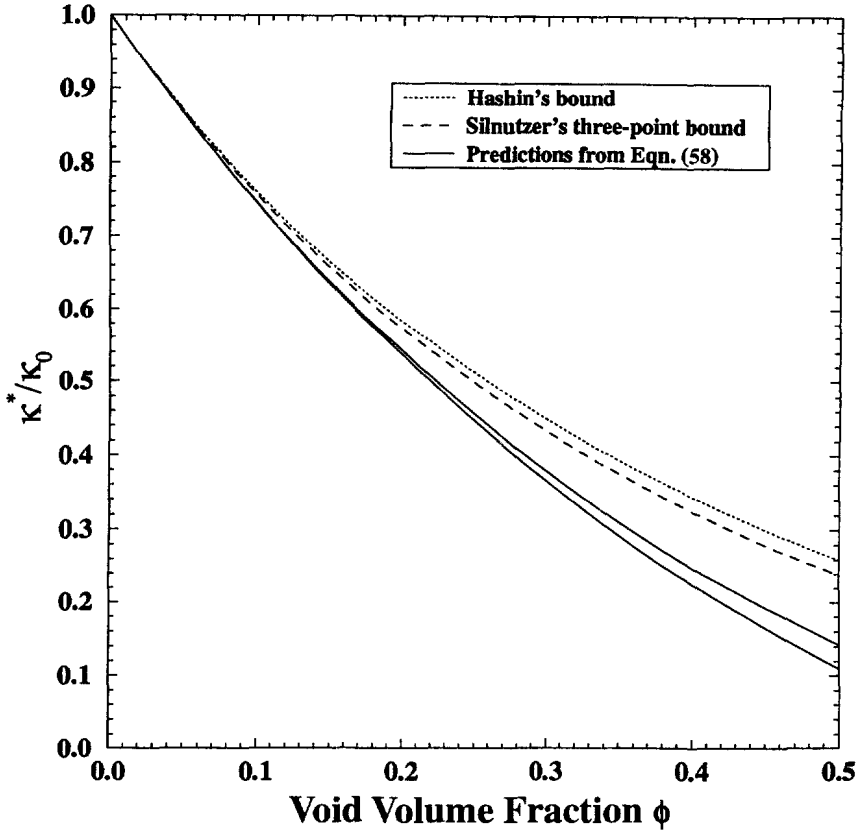

Fig. 6. The effective plane-strain bulk modulus vs. the void volume fraction ϕ for porous materials containing aligned cylindrical voids. The lower and upper solid lines correspond to the present method with the equilibrium and uniform RDFs, respectively.

the inclusion phase. We shall assume that $E_0 = 0.75 \times 10^6$ bars and $v_0 = 0.23$ for the glass matrix. Figure 6 compares the analytical predictions of the effective (normalized) plane-strain bulk modulus κ^*/κ_0 produced by the Hashin's (1965) upper bound, Silnutzer's (1972) 3-point upper bound, and the proposed method (by using the uniform and equilibrium RDFs). No available experimental data are found at this time for comparison.

As indicated by Christensen (1993), the manufacturing operations for fiber composite materials often involve the flow behavior of the composite system as viscous fluid suspensions. The matrix phase is usually treated as *incompressible* in its fluid state, and the aligned fibers are treated as *rigid* (in comparison with the matrix). Therefore, the (rheological) effective transverse shear viscosity η_T^* of these composite melts can be represented by the proposed eqn (63), with μ_T^* and μ_0 replaced by η_T^* and η_0. Figure 7 compares the theoretical predictions from Hashin's (1965) lower bound, Silnutzer's (1972) three-point lower bound (with the equilibrium RDF), Christensen's (1990, 1993) generalized self-consistent method (GSCM), and the proposed micromechanical interaction formulation (with the uniform and equilibrium RDFs). We observe that significant differences exist between our predictions and the other two bounds for ϕ greater than 30%. No experimental data are available in the open literature at this time for us to compare the analytical predictions. However, Ju and Chen (1994b) presented detailed experimental comparisons against the authors' micromechanical interaction formulation, the three-point lower bounds, and other methods for the effective shear viscosity vs. the particle volume fraction ϕ of colloidal suspensions containing an incompressible fluid matrix and randomly dispersed spherical rigid particles. Ju and Chen (1994b, Figure 6) showed that their micromechanical interaction formulation performed quite well while the three-point bound predictions did not fare well for ϕ greater than 30% in the colloidal suspensions. Although different in values, Christensen's (1990, 1993) predictions exhibit similar trend as our analytical predictions concerning effective shear viscosities η_T^* vs ϕ of circular fibers or spherical particles.

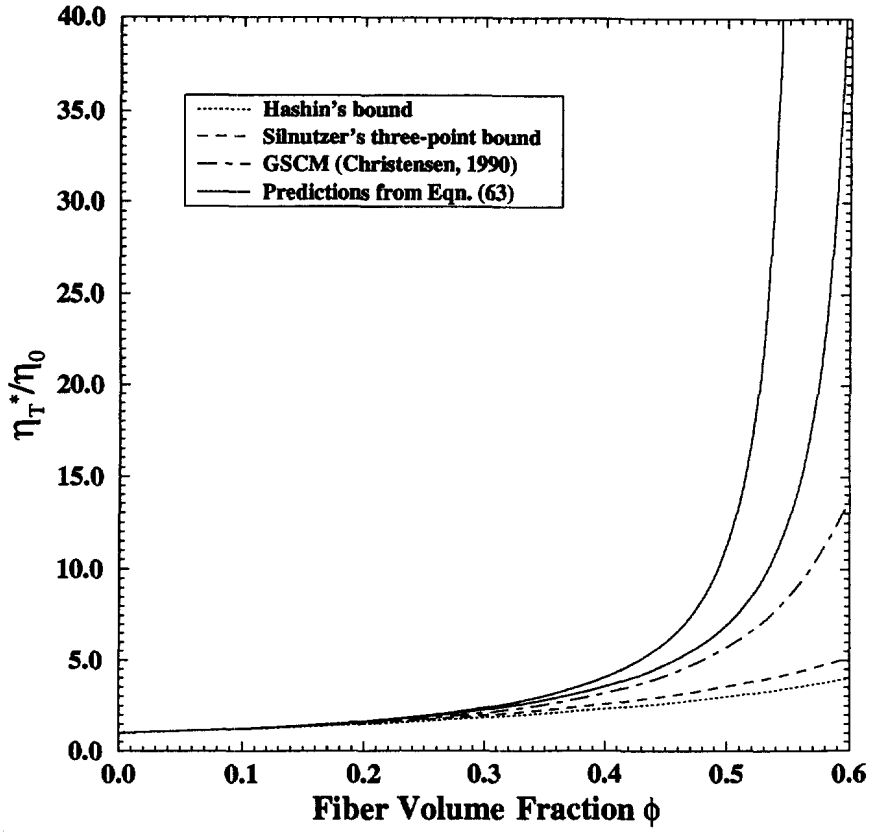

Fig. 7. The effective relative transverse shear viscosity vs. the fiber volume fraction ϕ. The upper and lower solid lines correspond to the present method with the equilibrium and uniform RDFs, respectively.

6. CONCLUSION

Based on the governing micromechanical field equations and the approximate pairwise fiber interaction solutions, a new micromechanical ensemble-area average approach is presented to predict effective transverse elastic moduli of linear two-phase composites containing randomly located yet aligned circular fibers. The proposed framework can be modified to accommodate circular fibers of different sizes and/or elastic properties. The ensemble-area averaged eigenstrains in fibers are approximately evaluated by eqn (36) or (47) through the pairwise inter-fiber interactions. Hence, a compact analytical formula (57) is derived. The proposed closed-form predictions are compared with Hashin's (1965) two-point bounds, Silnutzer's (1972) three-point bounds, and some available experimental data. These comparisons and simulations encompass fiber reinforced elastic composites, elastic matrix with randomly located cylindrical voids, and aligned viscous fiber suspensions. No Monte Carlo simulations nor finite element calculations are needed in the proposed framework.

The authors are currently working on the extension of the proposed method to predict the effective *elastoplastic* behavior of two-phase ductile matrix composites containing unidirectionally aligned yet randomly located elastic fibers. The methods proposed by Ju and Chen (1994c) and Ju and Tseng (1996, 1997) will be adopted to provide micromechanical ensemble-area averaged estimates.

Acknowledgements—This work was sponsored by the CUREe-Kajima Phase II Research Project under Grant D950217 (KaTRI Monitors: Dr Y. Nojiri and Mr Y. Nobuta; CUREe Monitor: Professor Wilfred D. Iwan), and by the National Science Foundation, Mechanics and Materials Program, under PYI Grant MSS-9157238 (Program Monitor: Dr Oscar W. Dillon). These supports are gratefully acknowledged. The authors are also indebted to Dr K. H. Tseng for his involvement and contributions during the early stage of this research.

REFERENCES

Budiansky, B. (1965) On the elastic moduli of some heterogeneous materials. *Journal of Mechanics and Physics of Solids*. **13,** 223–227.

Christensen, R. M. and Lo, K. H. (1979) Solutions for effective shear properties in three phase sphere and cylinder models. *Journal of Mechanics and Physics of Solids*, **27,** 315–330.

Christensen, R. M. (1990) A critical evaluation for a class of micro-mechanics models. *Journal of Mechanics and Physics of Solids*, **38,** 379–404.

Christensen, R. M. (1993) Effective viscous flow properties for fiber suspensions under concentrated conditions. *Journal of Rheology*, **37,** 103–121.

Eshelby, J. D. (1957) The determination of the elastic field of an ellipsoidal inclusion and related problems. *Proceedings of the Royal Society of London, Series A*, **241,** 376–396.

Hansen, J. P. and McDonald, I. R. (1986) *Theory of Simple Liquids*. Academic Press, New York.

Hashin, Z. and Rosen, B. (1964) The elastic moduli of fiber-reinforced materials. *Journal of Applied Mechanics*, **31,** 223–232.

Hashin, Z. (1965) On elastic behavior of fiber reinforced materials of arbitrary transverse phase geometry. *Journal of Mechanics and Physics of Solids*, **13,** 119–134.

Hashin, Z. (1972) Theory of fiber reinforced materials. NASA CR-1974, U.S.A.

Hashin, Z. (1983) Analysis of composite materials—a survey. *Journal of Applied Mechanics*, **50,** 481–505.

Hashin, Z. (1988) The differential scheme and its application to cracked materials. *Journal of Mechanics and Physics of Solids*, **36,** 719–734.

Hill, R. (1964) Theory of mechanical properties of fiber-strengthened materials—I. Elastic behavior. *Journal of Mechanics and Physics of Solids*, **12,** 199–212.

Hill, R. (1965) A self-consistent mechanics of composite materials. *Journal of Mechanics and Physics of Solids*, **13,** 213–222.

Honein, E. (1991) Multiple inclusions in elastostatics. Ph.D. dissertation, Department of Mechanical Engineering, Stanford University, Stanford, CA.

Honein, E., Honein, T. and Herrmann, G. (1992) Further aspects of the elastic field of two circular inclusions in antiplane elastostatics. *Journal of Applied Mechanics*, **59,** 774–779.

Honein, T., Honein, E. and Herrmann, G. (1994a) Circularly cylindrical and plane layered media in antiplane elastostatics. *Journal of Applied Mechanics*, **61,** 243–249.

Honein, E., Honein, T. and Herrmann, G. (1994b) Aspects of heterogenization. *Journal of Applied Mechanics*, **116,** 298–304.

Ju, J. W. and Chen, T. M. (1994a) Micromechanics and effective moduli of elastic composites containing randomly dispersed ellipsoidal inhomogeneities. *Acta Mechanica*, **103,** 103–121.

Ju, J. W. and Chen, T. M. (1994b) Effective elastic moduli of two-phase composites containing randomly dispersed spherical inhomogeneities. *Acta Mechanica*, **103,** 123–144.

Ju, J. W. and Chen, T. M. (1994c) Micromechanics and effective elastoplastic behaviour of two-phase metal matrix composites. *Journal of Engineering Materials and Technology, ASME*, **116,** 310–318.

Ju, J. W. and Tseng, K. H. (1996) Effective elastoplastic behavior of two-phase ductile matrix composites: A micromechanical framework. *International Journal of Solids & Structures*, **33,** 4267–4291.

Ju, J. W. and Tseng, K. H. (1997) Effective elastoplastic algorithms for ductile matrix composites. *Journal of Engineering*, **123,** 260–266. ASCE.

Kondo, K. and Saito, N. (1986) The influence of random fiber packing on the elastic properties of unidirectional composites. In *Composites '86: Recent Advances in Japan and the United States*, Proc. Japan-U.S. CCM-III, Tokyo.

Kouris, D. and Tsuchida, E. (1991) On the elastic interaction between two fibers in a continuous fiber composite under thermal loading. *Mechanics of Materials*, **12,** 131–146.

Kröner, E. (1958) Berechnung der elastischen Konstanten des Vielkristalls aus den Konstanten des Einkristalls. *Z. Phys.* **151,** 504–518.

Mallick, P. K. (1993) *Fiber-reinforced Composites: Materials, Manufacturing, and Design*. Marcel Dekker, Inc.

McLaughlin, R. (1977) A study of the differential scheme for composite materials. *International Journal of Engineering Science*, **15,** 237–244.

Milton, G. W. (1982) Bounds on the elastic and transport properties of two-component composites. *Journal of Mechanics and Physics of Solids*, **30,** 177–191.

Mori, T. and Tanaka, K. (1973) A average stress in a matrix and average elastic energy of materials with misfitting inclusions. *Acta Metallurgica*, **21,** 571–574.

Mura, T. (1987) *Micromechanics of Defects in Solids*, Second revised edition. Martinus Nijhoff Publishers, Dordrechet.

Nemat-Nasser, S. and Hori, M. (1993) *Micromechanics: Overall Properties of Heterogeneous Materials*. Elsevier Science Publisher B. V., The Netherlands.

Nomura, S. and Chou, T.-W. (1984) Bounds for elastic moduli of multiphase short-fiber composites. *Journal of Applied Mechanics*, **51,** 540–545.

Qiu, Y. P. and Weng, G. J. (1990) On the application of Mori-Tanaka's theory involving transversely isotropic spheroidal inclusions. *International Journal of Engineering Science*, **28,** 1121–1137.

Shioya, S. (1971) On the tension of an infinite thin plate containing a pair of circular inclusions. *Bulletins of the Japan Society of Mechanical Engineers*, **14,** 117–126.

Silnutzer, N. (1972) Effective constants of statistically homogeneous materials. Ph.D. thesis, University of Pennsylvania, Philadelphia, PA.

Taya, M. (1981) On stiffness and strength of an aligned short-fiber reinforced composite containing penny-shaped cracks in the matrix. *Journal of Composite Materials*, **15,** 198–210.

Taya, M. and Mura, T. (1981) On stiffness and strength of an aligned short-fiber reinforced composite containing fiber-end cracks under uniaxial applied stress. *Journal of Applied Mechanics*, **48,** 361–367.

Torquato, S. and Lado, F. (1992) Improved bounds on the effective elastic moduli of random arrays of cylinders. *Journal of Applied Mechanics*, **59,** 1–6.

Uemura, M. *et al.*, (1968) On the stiffness of filament wound materials (in Japanese). *Rep. Institute of Space and Aeronautical Science*, **4,** 448–463.
Weng, G. J. (1984) Some elastic properties of reinforced solids, with special reference to isotropic ones containing spherical inclusions. *International Journal of Engineering Science*, **22,** 845–856.
Weng, G. J. (1990) The theoretical connection between Mori-Tanaka's theory and the Hashin-Shtrikman-Walpole bounds. *International Journal of Engineering Science*, **28,** 1111–1120.
Zhao, Y. H., Tandon, G. P. and Weng, G. J. (1989) Elastic moduli for a class of porous materials. *Acta Mechanica* **76,** 105–131.
Zhao, Y. H. and Weng, G. J. (1990) Effective elastic moduli of ribbon-reinforced composites. *Journal of Applied Mechanics*, **57,** 158–167.

APPENDIX A: PLANE STRAIN ESHELBY'S TENSOR FOR A CIRCULAR INCLUSION

According to the Eshelby's solution, the elastic displacement field due to inclusion in an isotropic infinite body reads

$$u_i(\mathbf{x}) = -C_{jkmn}\varepsilon^*_{mn}\int_\Omega G_{ij,k}(\mathbf{x}-\mathbf{x}')\,d\mathbf{x}' \tag{74}$$

where the second rank plane-strain Green's function is given by Mura (1987):

$$G_{ij}(\mathbf{x}-\mathbf{x}') = \frac{1}{8\pi(1-\nu_0)\mu_0}\left[\frac{(x_i-x_i')(x_j-x_j')}{\|\mathbf{x}-\mathbf{x}'\|^2} - (3-4\nu_0)\delta_{ij}\ln\|\mathbf{x}-\mathbf{x}'\|\right]. \tag{75}$$

By taking the derivative of $G_{ij}(\mathbf{x}-\mathbf{x}')$ in eqn (75) with respect to x_k and substituting the result into eqn (74), we arrive at

$$u_i(\mathbf{x}) = -\frac{\varepsilon^*_{jk}}{4\pi(1-\nu_0)}\int_0^{2\pi} g_{ijk}(\mathbf{l})\frac{d\mathbf{x}'}{\|\mathbf{x}'-\mathbf{x}\|} \tag{76}$$

where

$$g_{ijk}(\mathbf{l}) = (1-2\nu_0)(\delta_{ij}l_k+\delta_{ik}l_j-\delta_{jk}l_i)+2l_il_jl_k \tag{77}$$

and $\mathbf{l}\equiv(\mathbf{x}'-\mathbf{x})/\|\mathbf{x}'-\mathbf{x}\|$. When the point $\mathbf{x}$ is located inside the inclusion, the strain and stress fields become uniform for the interior points. Moreover, eqn (76) can be integrated explicitly. The differential element $d\mathbf{x}'$ can be written as

$$d\mathbf{x}' = r\,dr\,d\theta \tag{78}$$

where $r = \|\mathbf{x}'-\mathbf{x}\|$ and $d\theta$ is the differential angle centered at point $\mathbf{x}(x_1, x_2)$; see Fig. 8 for a schematic plot of a circular inclusion. Upon integration with respect to r, eqn (76) becomes

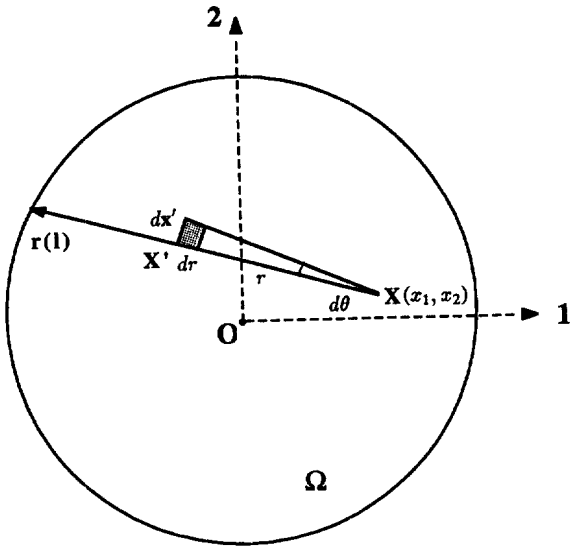

Fig. 8. The domain of a fiber cross-section Ω.

$$u_i(\mathbf{x}) = -\frac{\varepsilon^*_{jk}}{4\pi(1-\nu_0)}\int_0^{2\pi} r(\mathbf{l})g_{ijk}(\mathbf{l})\,\mathrm{d}\theta. \tag{79}$$

Here, $r(\mathbf{l})$ is the positive root of the following equation

$$(x_1+rl_1)^2+(x_2+rl_2)^2 = a^2. \tag{80}$$

Therefore, we have

$$r(\mathbf{l}) = -\frac{f}{h}+\sqrt{\frac{f^2}{h^2}+\frac{e}{h}} \tag{81}$$

where

$$h = \frac{l_1^2+l_2^2}{a^2} \tag{82}$$

$$f = \frac{l_1x_1+l_2x_2}{a^2} \tag{83}$$

$$e = 1-\frac{x_1^2+x_2^2}{a^2}. \tag{84}$$

Substituting eqn (81) into eqn (79), we find that the integration involving the $\sqrt{f^2/h^2+e/h}$ term vanishes because it is even in $\mathbf{l}$ while g_{ijk} is odd in $\mathbf{l}$. Consequently, we obtain

$$u_i(\mathbf{x}) = \frac{x_j\varepsilon^*_{mn}}{4\pi(1-\nu_0)}\int_0^{2\pi}\frac{\lambda_j g_{imn}(\mathbf{l})}{h}\,\mathrm{d}\theta \tag{85}$$

and

$$\varepsilon_{ij}(\mathbf{x}) = \frac{\varepsilon^*_{kl}}{8\pi(1-\nu_0)}\int_0^{2\pi}\frac{\lambda_i g_{jkl}+\lambda_j g_{ikl}}{h}\,\mathrm{d}\theta \tag{86}$$

where

$$\lambda_i \equiv l_i/a^2. \tag{87}$$

According to the definition of Eshelby's tensor $\varepsilon_{ij} = s_{ijkl}\varepsilon^*_{kl}$, we then arrive at

$$s_{ijkl} = \frac{1}{8\pi(1-\nu_0)}\int_0^{2\pi}\frac{\lambda_i g_{jkl}-\lambda_j g_{ikl}}{h}\,\mathrm{d}\theta. \tag{88}$$

Finally, the plane-strain Eshelby's tensor for a circular inclusion can be expressed as

$$s_{ijkl} = \frac{1}{8\pi(1-\nu_0)}[(4\nu_0-1)\delta_{ij}\delta_{kl}+(3-4\nu_0)(\delta_{ik}\delta_{jl}+\delta_{il}\delta_{jk})]. \tag{89}$$

APPENDIX B: THE INVERSE OF A FOURTH-RANK TENSOR F

The product between two 2-D fourth-rank tensors $\mathbf{F}(A_m)$ and $\mathbf{F}(B_m)$, $m = 1$ to 6, can be shown to follow

$$F_{ijpq}(A_m)F_{pqkl}(B_m) = F_{ijkl}(C_m) \tag{90}$$

where $i, j, k, l, p, q = 1, 2$, $\mathbf{F}$ is defined in (5), and

$$C_1 = A_1(B_1+4B_2+B_3+2B_6)+4A_2(B_1+2B_2+B_3)+A_4(B_1+4B_2+2B_3)+2A_6B_1 \tag{91}$$

$$C_2 = 2A_2(B_2+B_6)+2A_6B_2 \tag{92}$$

$$C_3 = A_3(B_1+4B_2+B_3+2B_6)+A_5(B_1+4B_2+2B_3)+2A_6B_3 \tag{93}$$

$$C_4 = A_1(B_4+B_5)+4A_2(B_4+B_5)+A_4(B_4+2B_5+2B_6)+2A_6B_4 \tag{94}$$

$$C_5 = A_3(B_4+B_5)+A_5(B_4+2B_5+2B_6)+2A_6B_5 \tag{95}$$

$$C_6 = 2A_6B_6. \tag{96}$$

One should note that the tensorial product of $\mathbf{F}(A_m)$ and $\mathbf{F}(B_m)$ does not commute in general, i.e.,

$$\mathbf{F}(A_m)\cdot\mathbf{F}(B_m) \neq \mathbf{F}(B_m)\cdot\mathbf{F}(A_m). \tag{97}$$

To find the inverse of $\mathbf{F}$, we first recall the definition of the fourth-rank unit tensor:

$$I_{ijkl} \equiv \tfrac{1}{2}(\delta_{ik}\delta_{jl}+\delta_{il}\delta_{jk}). \tag{98}$$

Denoting now by $\mathbf{F}(A_m)$ the inverse tensor of $\mathbf{F}(B_m)$, we can derive the components of $\mathbf{F}(A_m) \equiv \mathbf{F}^{-1}(B_m)$ by solving the system of eqns (91)–(96) with the following arguments in $\mathbf{F}(C_m)$:

$$C_1 = C_2 = C_3 = C_4 = C_5 = 0, \quad C_6 = \tfrac{1}{2}. \tag{99}$$

The results are

$$A_6 = \frac{1}{4B_6} \tag{100}$$

$$A_2 = -\frac{B_2}{4B_6(B_2+B_6)} \tag{101}$$

and

$$\begin{Bmatrix} A_1 \\ A_4 \end{Bmatrix} = \mathbf{D}^{-1}\begin{Bmatrix} -2A_6B_1-4A_2(B_1+2B_2+B_3) \\ -2A_6B_4-4A_2(B_4+B_5) \end{Bmatrix} \tag{102}$$

$$\begin{Bmatrix} A_3 \\ A_5 \end{Bmatrix} = \mathbf{D}^{-1}\begin{Bmatrix} -2A_6B_3 \\ -2A_6B_5 \end{Bmatrix} \tag{103}$$

where

$$\mathbf{D} \equiv \begin{bmatrix} B_1+4B_2+B_3+2B_6 & B_1+4B_2+2B_3 \\ B_4+B_5 & B_4+2B_5+2B_6 \end{bmatrix}. \tag{104}$$